Effect of Moisture and Orientation on the Fracture of Nylon 6,6 Fibers

S. MICHIELSEN

DuPont Nylon, Experimental Station, Wilmington, Delaware 19880-0302

SYNOPSIS

The effect of relative humidity on the fracture of single nylon 6,6 fibers is determined using fracture mechanics. The fracture energy release rate, G_{Ic}, of these fibers is shown to be 8× that for injection-molded nylon 6,6 at 0% RH. G_{Ic} varies from 31.3 kJ/m^2 at 0% RH to 15.6 kJ/m^2 at 100% RH. The dependence of G_{Ic} on RH is in agreement with previous studies indicating two types of water in nylon: a tightly bound and a loosely bound type. In addition, G_{Ic} is shown to be 10× greater for transverse fiber breaks than for axial splitting of the fiber due to the high degree of orientation in these fibers. These studies are the first of their kind for organic fibers. © 1994 John Wiley & Sons, Inc.

INTRODUCTION

The effects of moisture on the mechanical properties of nylon have been studied for the last 50 years. Papir et al.[1] reviewed such a study on nylon 6. Likewise, the effect of orientation on the strength and modulus of nylon fibers has been studied nearly this long. To date, a solid understanding on how moisture and orientation affects the strength of nylon fibers is not yet in hand.

Papir et al.[1] found that there were two types of water in nylon 6: a tightly bound portion that interrupts the hydrogen bonds between amide groups on neighboring chain segments by forming water bridges between them, and a second, loosely bound water that acts primarily as a diluent. Both of these types of water exist exclusively in the amorphous regions. It is believed that all the water exists as tightly bound water until nearly all the amide–amide hydrogen bonds have been replaced by the tightly bound water bridges in the form of amide–water–amide hydrogen bonds. Thereafter, the water is absorbed in the loosely bound form. Due to the similarities between nylon 6,6 and nylon 6, it is believed that water in nylon 6,6 behaves in a similar manner.

Likewise, many attempts to understand the failure of fibers have been made. In most of these, an analysis of inherent flaw sizes has been made, although actual flaw sizes have not generally been measured. Instead, elaborate statistical analyses have been performed to predict the failure. In other areas of science, fracture mechanics (FM) has been successfully applied to predicting failure of materials when flaws of known size are present following the classic work of Griffith[2] more than 70 years ago in which he described the failure of glass bulbs and tubes. During the intervening years, FM has been successfully applied to describe fracture of metals, ceramics, glasses, composites, plastics, and elastomers.

When Griffith originally developed FM for glass, he found that the fracture energy was just that required to create new surface area, i.e., the surface free energy of glass times the fracture area. For most other materials, it has since been found that the energy required to propagate a crack greatly exceeds the surface free energy. This has been attributed to a damage zone around the crack tip, rather than just a crack plane. Since a significant volume of material may be involved in this damage zone, the fracture energy is often orders of magnitude larger than the surface free energy. From a practical point of view, if the sample dimensions greatly exceed the size of the damage zone, then the size of the damage zone and the energy required to create it will depend only on material properties and not on the test geometry. Thus, the formalism of FM can still be used provided

Journal of Applied Polymer Science, Vol. 52, 1081–1089 (1994)
 CCC 0021-8995/94/081081-09

that we interpret the fracture energy not as a surface energy alone but also include the energy required to create and propagate the damage zone. This energy is often referred to as the fracture energy release rate per unit crack area, or G_{Ic} for plane strain or mode I fractures.

Because of the restriction that the specimen size must be much greater than the damage zone size to be a valid fracture test, several criteria have been developed to determine the minimum specimen size. For a single-edge notch in three-point bending, the ASTM size criteria for a valid test is given as[3]

$$x \geq 2.5(K_{Ic}/\sigma_y)^2 \quad (1)$$

where x is the smallest of the width, the thickness, the crack length, or the width minus the crack length. K_{Ic} is the stress intensity factor [$= (G_{Ic}E)^{1/2}$, where E is Young's modulus] and σ_y is the yield stress. Adams et al.[4] gave $K_{Ic} = 3.7$ MPa $m^{1/2}$ and $\sigma_y = 82$ MPa (Ref. 5) for dry as molded (DAM) nylon 6,6 injection-molded bars, so that $x \geq 5$ mm. For other test geometries, similar damage zone sizes are expected and, thus, similar size criteria are expected. It is not surprising then that FM has not previously had much success in describing the fracture of polymer-based fibers since their largest dimension, other than length, is far smaller than 5 mm.

Studies of the moisture sensitivity of crack growth rates in injection-molded nylon 6,6 were performed by Bretz et al.,[6] but they did not determine critical values of G_{Ic} or K_{Ic}. They found that the fatigue crack growth rate depended strongly on RH with a minimum in the growth rate at a water content of about 2.5% (RH $\approx$ 50%) and similarly for nylon 6. This is exactly where Papir et al. found the boundary between the tightly bound water and the loosely bound water. Bretz et al. attributed this minimum in crack growth rate as an optimization between crack blunting and loss of modulus. Karger-Kocsis and Friedrich[7] also studied the effects on RH on the fatigue crack growth rates. They found that although the crack growth rates depended strongly on RH the critical values, K_{Ic}, were independent of RH. They studied only two RH values—dry and 100%, and thus did not observe a minimum in crack growth rates with RH.

Karger-Kocsis and Friedrich[7] also studied the effect of orientation relative to the mold-filling direction (MFD) on fatigue crack growth rates, finding only slight differences between the crack growth rates for crack propagation parallel to the MFD vs. those propagating perpendicular to MFD. However, the relative orientation in injection-molded samples is far smaller than that in the highly drawn fibers in the current study.

Recently, Michielsen[8] showed that FM could be successfully applied to single nylon 6,6 monofilaments whose dimensions were less than 1 mm. These fibers had been drawn well beyond their primary yield point during the manufacturing process and no subsequent yielding was observed below their breaking stress; rather, they failed brittlely. Another feature of drawn fibers is that they are highly anisotropic, as shown by birefringence and X-ray measurements. When FM has been applied to anisotropic fibrous composite materials, fractures in different directions have markedly different G_{Ic}'s. Similar behavior might be expected for an oriented fiber, but it is generally impossible to measure the strength of a fiber for breaks parallel to their axis since they are too thin to grip in a testing machine.

This article continues the study discussed in Ref. 8 in describing the use of FM to measure G_{Ic} of single nylon 6,6 fibers. Herein is reported G_{Ic} for fractures both perpendicular to and parallel with the fiber axis. Also reported is the dependence of G_{Ic} on RH. These studies are the first of this kind on single, organic polymer fibers.

EXPERIMENT

The samples used in this study were Hyten nylon 6,6 monofilaments. (Hyten is a registered trademark of the E. I. DuPont Co.) Two different size fibers were used: 2110 and 6400 denier fibers. These fibers are nearly rectangular but with semicircular ends (see Ref. 8). The approximate dimensions are shown in Table I as are the crystal orientations, determined from the half-width at half-maximum (hwhm) of the 100 peak in the X-ray diffraction pattern. This gives the angular spread of the crystal orientation and indicates that these fibers are very highly oriented.

Fibers were notched by one of two methods; both methods used a fresh razor blade for each notch. For

Table I Fiber Dimensions and Orientation

Denier	Thickness (μm)	Width (μm)	Orientation Angle (Degrees)	$G_{Ic}^{\perp}$ 65% RH (kJ/m^2)
2110	260	840	9.2	17.0
6397	460	1460	9.5	17.0

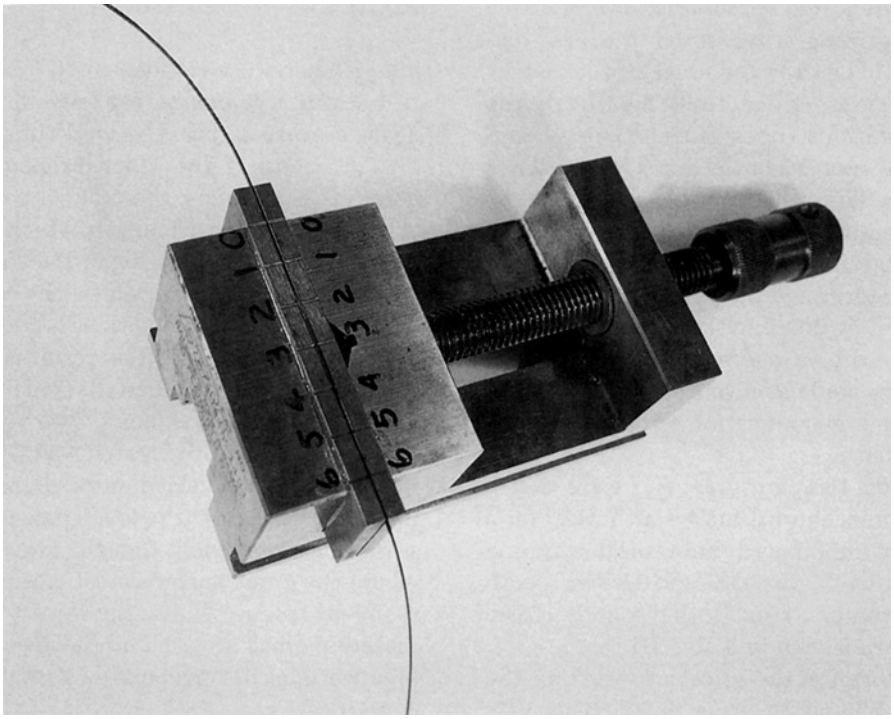

Figure 1 A fiber is mounted in the notching jig such that the top edges of the fiber and the jig coincide. A fresh razor blade is then drawn through one of the slots numbered 0–6 to notch the fiber. Each notch is of a different depth. Note that the fiber has been artificially colored black for clarity.

measurements of G_{Ic} for a crack opening parallel to the fiber axis or axial splitting, the notch was made by carefully pushing the razor blade into the end of the fiber. The two sides were then pulled apart until the crack reached a length convenient for mounting in an Instron tensile testing machine, or approximately 2.5 cm, and $G_{Ic}^{\parallel}$ was determined. For measurements of G_{Ic} for cracks running perpendicular to the fiber axis or transverse cracks, the fiber was mounted in a special jig that consisted of a smooth jawed vise with notches of various depths machined into the top of the jaws (see Fig. 1). The fibers were mounted with the top edge of the fiber coinciding with the top edge of the vise jaws. A razor blade was then drawn through the appropriate notch in the vise jaw to make a comparable size notch in the fiber. The notch depth in the fiber was determined after testing by examining the fracture surface using a scanning electron microscope (SEM) and, finally, $G_{Ic}^{\perp}$ was determined.

After notching, the samples were conditioned to the desired RH. Dry fibers were found to have reached equilibrium moisture content in 100% RH after 24 h. Likewise, these water-saturated fibers were found to reach equilibrium at 0% RH in less than 48 h in a vacuum at room temperature. Based on these results, a minimum equilibration time of 7 days was chosen. The 50% RH and 65% RH fibers were aged 1 week and tested in humidity-controlled rooms. The 100% RH fibers were immersed in water at room temperature for more than 1 week. They were quickly wiped dry and tested immediately afterward. The 22% RH fibers were conditioned for 1 week in a sealed chamber containing a saturated aqueous potassium acetate solution and removed just before testing. The 0% RH fibers were placed in a vacuum at room temperature and a pressure of less than 1 Torr for 1 week. They were then transferred to a desiccator for an additional week and removed from the desiccator just before testing.

All samples were tested in a computerized Instron tensile testing instrument to facilitate data processing. For measurements of $G_{Ic}^{\perp}$, a 25.4 cm gauge length was used with flat grips and a strain rate of 10%/min. $G_{Ic}^{\perp}$ was measured with a very short gauge length and with a crosshead speed of 1.27 cm/min. Due to the different sample geometries, the same strain rates could not be used for both geometries.

To determine G_{Ic}, both the work to increase the crack area and the increase in crack area are re-

quired. The work required to increase the crack area is determined by integrating under the load-displacement curve. The area for cracks propagating along the fiber axis is estimated by measuring the crack length at various times during the test and assuming that the area is just the crack length times the sample width. The crack length was found to be equal to $\frac{1}{2}$ the crosshead displacement, as expected. For cracks propagating across the fiber, the initial crack area was determined by measuring the crack length as observed by imaging the fracture surfaces with a scanning electron microscope (SEM). Corrections were then made as discussed below for the fiber shape and for a magnification error in the SEM as described in Ref. 8.

Glass transition temperatures, T_g, were determined by thermomechanical analysis (TMA) on a TMA 2940 and by modulated differential scanning calorimetry (mod-DSC) on a DSC 2910 MDSC, both made by TA Instruments, Inc. Both methods agreed within 2°C and are shown in Table III.

Finally, to determine the effect of water on the extent of hydrogen bonding, cyclic tensile tests were performed on an Instron tensile testing machine. The fibers were mounted on the testing machine with a 25.4 cm gauge length. The fibers were then elongated at 10%/min to 10% strain and returned to their initial length, also at 10%/min. This was repeated immediately for a total of five times and the initial modulus was determined on the fifth cycle. The fibers were then allowed to relax for 24 h and then tested again, ensuring that the fibers were replaced exactly as they had been initially.

ANALYSIS

The geometry used to measure $G_{Ic}^{\parallel}$ is a simple tearing test. For this geometry, the energy required to propagate a crack is just the load times the crosshead displacement. If the crack propagates as a plane across the fiber axis, the crack area is just the fiber width times the crack length, which was determined above to be equal to $\frac{1}{2}$ the crosshead displacement. In the present case, however, the crack propagates along the fiber axis but with hills and valleys running along the fiber length. The result is that the area is actually much larger than that calculated by assuming the crack to be a plane. The variation in crack area as the crack propagated was also evident in the load trace, which varied markedly, as shown in Figure 2. On matching the load trace with the fracture surface, it was evident that the lowest loads occurred where the crack surface most closely approximated a smooth plane. Thus, the lowest load that could maintain crack growth and the lowest possible crack area were used to calculate $G_{Ic}^{\parallel}$ using the following equation[9]:

$$G_{Ic}^{\parallel} \leq \frac{P}{D} \tag{2}$$

where P is the load, and D, the fiber width. The minimum load was 1.4 Newtons, and the width, 840 μm; thus, $G_{Ic}^{\parallel} \leq 1.7$ kJ/m^2 at 65% RH and 21°C for the 2110 denier fiber.

Likewise, the method to determine $G_{Ic}^{\perp}$ is a simple tensile test on a notched fiber. The analysis is more

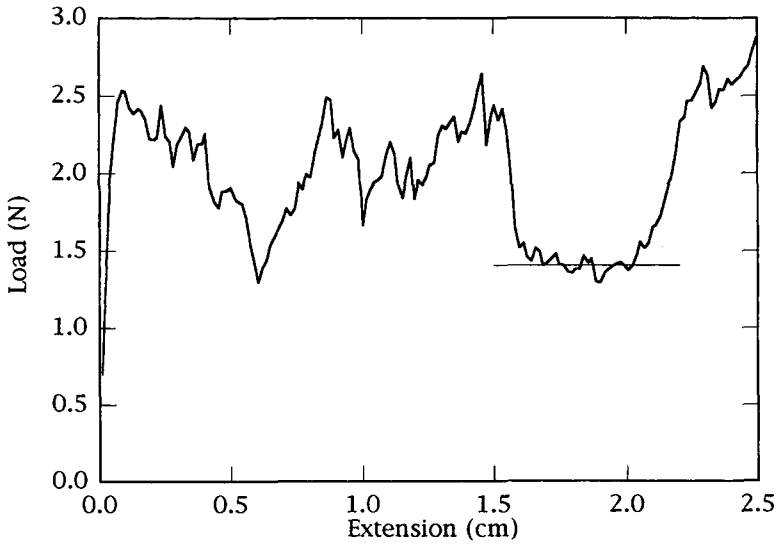

Figure 2 Load trace for along axis tear. The horizontal line shows the load used to determine $G_{Ic}^{\parallel}$. This corresponds to the smoothest region of the fracture surface.

complicated, however, as described in Refs. 8 and 10. In this case,

$$G_{Ic}^{\perp} = \frac{2\pi W_0}{\lambda^{1/2}} \frac{25a_0}{20 - 13\frac{a_0}{D} - 7\left(\frac{a_0}{D}\right)^2} \quad (3)$$

where $\lambda = L/L_0$ is the extension ratio; L, the length at break; L_0, the initial length; a_0, the initial crack length, and D, the sample width. W_0 is the strain energy density determined by integrating the load-displacement curve to get the energy to break and dividing by the initial sample volume provided that all of the energy goes into elastic deformation of the sample, i.e., the sample does not yield. It is not necessary that the sample exhibits linear stress–strain behavior, only that the energy is stored elastically.

Equation (3) is valid for an infinitely long rectangular bar. Our length-to-width ratio, L/D, is ≥ 170, or nearly infinite. However, the fiber is not quite rectangular and a correction needs to be made. The correction that seems most appropriate is one in which the true crack area is equal to a crack of effective length a_0^{eff} in a rectangular bar of equal area and aspect ratio as the fiber. Thus, the crack area, A, is, for $a_0 \geq t/2$,

$$A = \frac{\pi}{2}\left(\frac{t}{2}\right)^2 + t\left(a_0 - \frac{t}{2}\right) \quad (4)$$

where t is the fiber thickness, and a_0, the true crack length. The effective crack length, a_0^{eff}, is

$$a_0^{\text{eff}} = \frac{A}{t^{\text{eff}}} = \frac{DA}{tA_{\text{fiber}}} \quad (5)$$

where A_{fiber} is the cross-sectional area of the fiber determined from the fiber denier and t^{eff} is the thickness of a rectangular bar with the same cross-sectional area and the same aspect ratio. This correction is small for all but the shortest cracks.

Measurements of the fiber width and thickness from SEM micrographs were found to be in error when compared to direct measurements with a micrometer and dimensions determined from the denier. Since a_0 was also determined from these micrographs, a further correction was required. The apparent crack length, a_{SEM}, and the apparent width, D_{SEM}, were measured in an SEM photomicrograph. The true width, D_{denier}, was determined by direct measurement and from the specimen denier. The true crack length was then determined:

$$a_0 = a_{\text{SEM}} \frac{D_{\text{denier}}}{D_{\text{SEM}}} \quad (6)$$

This value for the crack length was used in eqs. (4) and (5) to determine a_0^{eff}. Then, a_0^{eff} and the width of an equivalent rectangular bar, $D^{\text{eff}} = (A_{\text{fiber}}D/t)^{1/2}$, were substituted into eq. (3) to obtain $G_{Ic}^{\perp}$.

Figure 3 shows a plot from which $G_{Ic}^{\perp}$ was determined at 0% RH for the case where no shape correction is made and one in which the crack area is corrected as described above. The 25% discrepancy

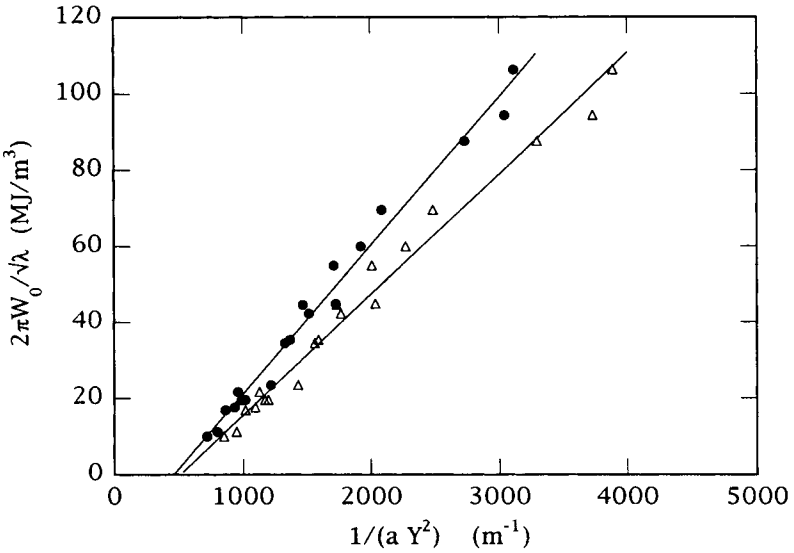

Figure 3 (●) No shape correction is made in determining $G_{Ic}^{\perp} = 39.4$ kJ/m^2; (△) the equal area shape correction described in the text is made, $G_{Ic}^{\perp} = 31.3$ kJ/m^2.

Table II Comparison of G_{Ic} for Fiber and Molded Plaque

	% RH	Orientation	Young's Modulus (GPa)	G_{Ic} (kJ/m^2)
This work	0	High	6.0	31.3
Adams et al.[4]	DAM	Low	2.7	3.9
		Ratio	2.2	8.0

between these values, $G_{Ic}^{\perp}$, shows the importance of correcting for the shape.

One test of the validity of fracture mechanics is that G_{Ic} must be independent of the sample size. Table I shows that there is no difference in $G_{Ic}^{\perp}$ between the 2110 denier and the 6400 denier fibers at 65% RH.

RESULTS

It is well known that by orienting a fiber the initial Young's modulus (E_i) increases in the direction of the draw. In the current study on highly oriented fibers, E_i was found to be 2.2× the Young's modulus of injection-molded bars in the study by Adams et al.[4] No similar study of the effect of orientation on G_{Ic} has previously been performed. Table II compares the results of this study with that of Adams et al.,[4] from which it is clear that G_{Ic} of the oriented fiber is 8× greater than that of the molded bar and the increase in G_{Ic} is almost 4× larger than the increase in E_i due to orientation. This suggests that a measurement of the anisotropy of G_{Ic} would be of great interest and is shown in Table III, where at 65% RH $G_{Ic}^{\perp}$ is more than 10× that of $G_{Ic}^{\parallel}$. Thus, the increase in $G_{Ic}^{\perp}$ due to orienting the fiber is accompanied by a decrease in $G_{Ic}^{\parallel}$. Although this anisotropy in strength has been suggested before, it has not previously been measured.

Another well-known fact is that E_i for nylon 6,6 fibers is quite sensitive to RH. Figure 4 shows the dependence of E_i and $G_{Ic}^{\perp}$ on RH. At 0% RH, the Young's modulus is 6.0 GPa and decreases gradually as RH is increased to 65%. Above 65% RH, E_i decreases rapidly, until at 100% RH, it has fallen to 1.7 GPa. In contrast, $G_{Ic}^{\perp}$ decreases rapidly from 0% RH to 50% RH and thereafter decreases only slightly. It is quite clear that E_i and $G_{Ic}^{\perp}$ have very different dependencies on RH and therefore must have different dependencies on the changes in the microstructure caused by the absorption of water.

On close examination of the stress–strain curves (Fig. 5) for these fibers, a pronounced hump is easily seen at low RH, whereas at higher RH, this hump nearly disappears. This hump can be attributed to hydrogen bonding between amide groups on adjacent chain segments in the amorphous regions. As the fibers are elongated, the hydrogen bonds at first restrict the motion of the chain segments, resulting in a higher modulus. On continued elongation, the H bonds break and the stress–strain curve returns to what it would have been in absence of the H bonds. At low RH, only inter- and intrachain H bonds are possible. As RH increases to 50% RH, some of the amide–amide H bonds between chain segments are gradually replaced by amide–water–amide H bonds that still restrict chain motions and the initial modulus remains high. Above 50% RH, the water goes in as the loosely bound form and plasticizes the amorphous regions, thus decreasing the modulus. Figure 6 shows hysteresis curves for 0% RH in which the initial hump seen in the first cycle nearly disappears by the fifth cycle, in agreement with the hypothesis that cycling the fiber to 10% strain should break most of the H bonds in the amorphous regions, resulting in a lower initial modulus. After waiting 24 h and retesting, the load-displacement curve returns to its initial shape, indicating that the changes are temporary as would be expected if the H bonds are broken since they can reform easily. This would not be the case, however,

Table III Summary of RH Dependence of $G_{Ic}^{\perp}$ and E_i

RH (%)	$G_{Ic}^{\perp}$ (kJ/m^2)	$G_{Ic}^{\parallel}$ (kJ/m^2)	E_i (GPa)	T_g (°C)	Intercept (mJ/m^3)
0	31.3		6.0	68.1	−15.2
22	27.7		5.8	64.9	−11.2
50	18.8		4.8	51.0	2.6
65	17.0	< 1.7	4.4	49.1	2.5
100	15.6		1.7	23.3	9.2

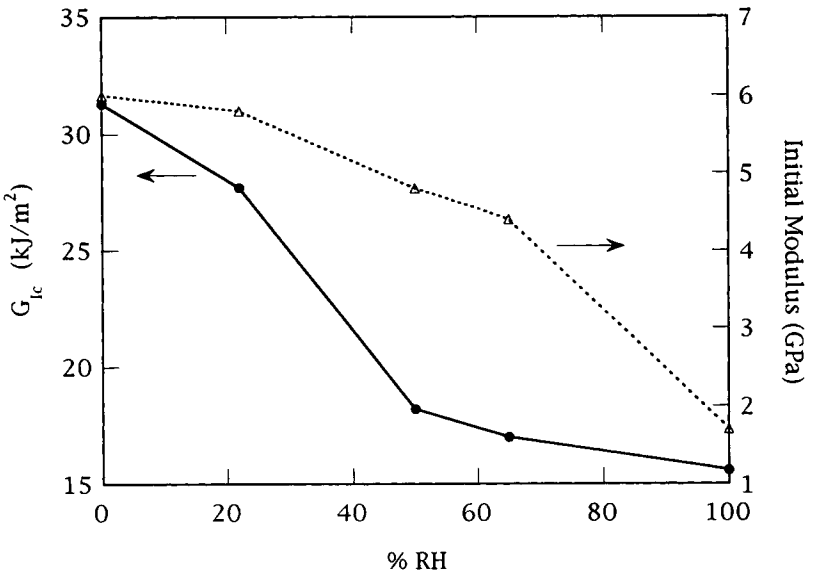

Figure 4 Comparison of the RH dependence (●) of $G_{Ic}^{\perp}$ and (△) of E_i.

if the polymer chains were broken by this process. In contrast, at 100% RH as shown in Figure 7, there is little difference between in the shape of the cycle 1 and cycle 5 load-displacement curves. This indicates that at 100% RH most of the inter- and intrachain H bonds have been disrupted by the water and thus are no longer restrictive of chain motion.

The fifth cycle initial moduli, E_i^{5th} are shown in Figure 8. It is clear from the linear decrease in modulus with % RH that a portion of the water acts as a plasticizer, merely reducing the modulus. This is what Papir et al.[1] refer to as the loosely bound water. The remainder of the water is the tightly bound water that inserts itself into the H bonds between neighboring amides to form amide–water–amide H bonds.

The $G_{Ic}^{\perp}$ dependence on RH is now understandable. Following Papir et al.,[1] the water initially goes into the amorphous region of nylon 6,6 primarily as tightly bound water to form amide–water–amide H

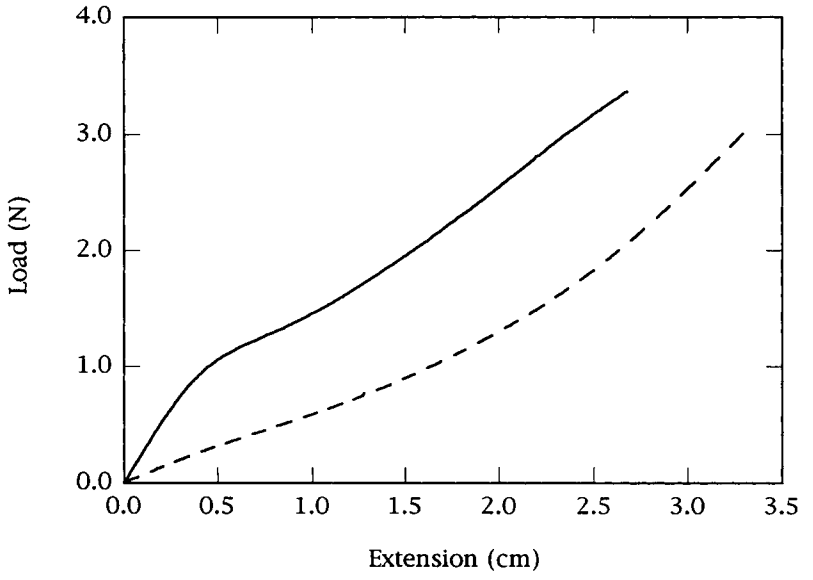

Figure 5 Load-displacement curves: (——) at 0% RH; (- - -) at 100% RH.

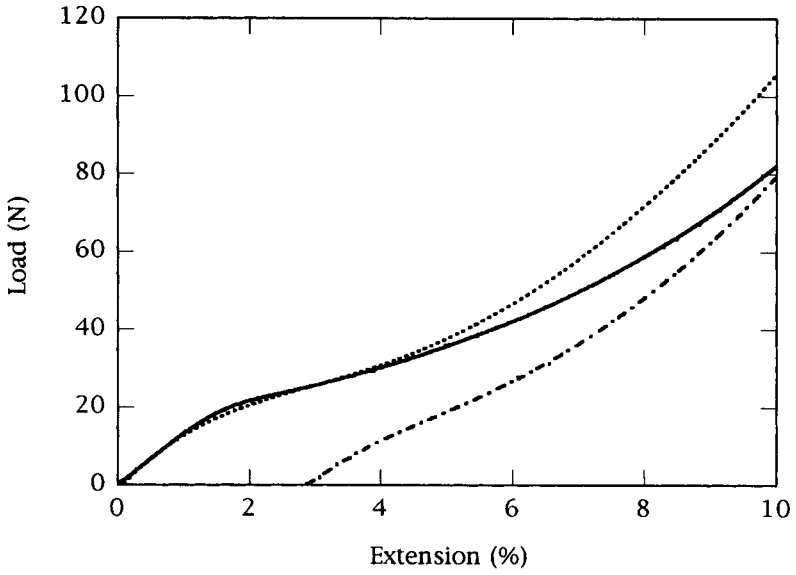

Figure 6 (——) First cycle; (– · –) fifth cycle; (- - - -) first cycle after 24 h recovery load-displacement curves at 0% RH.

bonds. When nearly all of the amide–amide H bonds have picked up water, at about 50% RH, the additional water acts purely as a diluent. Thus, initially $G_{Ic}^{\perp}$ decreases nearly linearly with RH as the amide–amide H bonds are replaced by amide–water–amide H bonds, which presumably require less energy to break than do the amide–amide H bonds. Once all the amide–amide H bonds have been replaced, $G_{Ic}^{\perp}$ remains nearly constant since there are no further structural changes in the polymer. The remaining water does, however, act as a diluent.

There remains one difficulty with the fracture analysis above as shown in the last column in Table III. The plots in Figure 3 should pass through the origin since it should require zero work to "break" a fiber that has been cut all the way through. The

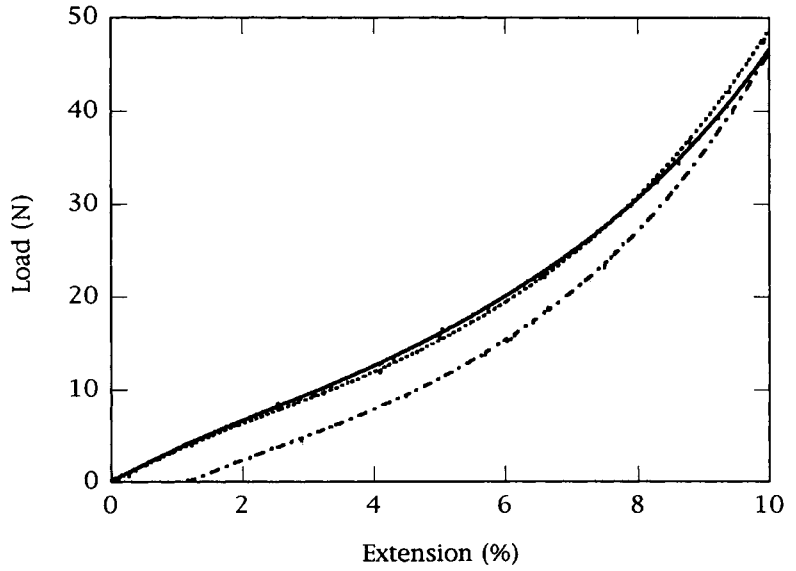

Figure 7 (——) First cycle; (– · –) fifth cycle; (- - - -) first cycle after 24 h recovery load-displacement curves at 100% RH.

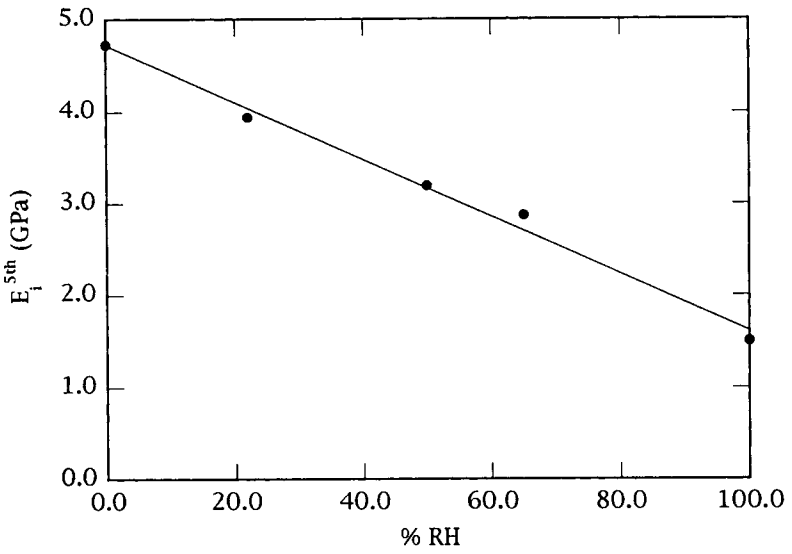

Figure 8 RH dependence of the fifth cycle initial moduli, E_i^{5th}.

intercepts given in Table III indicate that this is not the case here! It is conceivable that there are residual internal stresses, the magnitude of which depends on the RH. These stresses would add to the applied stress, thus shifting the intercepts. Nevertheless, the exact interpretation of these intercepts is still an open question at this time.

CONCLUSIONS

Fracture mechanics has been shown to describe the fracture of single nylon 6,6 fibers. The dependence of $G_{Ic}^{\perp}$ on relative humidity has been determined and shown to agree with previous studies, indicating the presence of two types of water, a tightly bound water and a loosely bound water, in nylon. In addition, it was shown that these fibers exhibit markedly different G_{Ic}'s in different directions. Although this is anticipated based on fracture studies of unidirectional fiber-reinforced composites, it has not previously been demonstrated within a single fiber. The high degree of orientation of these fibers greatly increases $G_{Ic}^{\perp}$ over G_{Ic} for an unoriented plaque. Further experiments on smaller fibers are in progress.

The author would like to thank J. G. Williams, D. D. Huang, and B. A. Crouch for providing guidance in the proper FM procedures, D. G. Clemens for preparing the samples and determining the initial crack lengths, K. T. Mardecz for measuring the hysteresis curves, C. C. Zimmerman and I. R. Craighead for measuring the stress/strain curves of the notched fibers, C. S. Chaplow and J. M. Heitur for taking the SEM micrographs, and R. A. Twadell for measuring the T_g's.

REFERENCES

1. Y. S. Papir, S. Kapur, C. E. Rogers, and E. Baer, *J. Polym. Sci. A-2,* **10,** 1305 (1972).
2. A. A. Griffith, *Philos. Trans. R. Soc.,* **A221,** 163–198 (1920).
3. ASTM Standards, **31** 1099–1114 (1969); W. F. Brown, Ed., *Review of Developments in Plane Strain Fracture Toughness Testing,* ASTM Special Technical Publication 463, American Society for Testing and Materials, Lutherville, MD, 1970.
4. G. C. Adams, R. G. Bender, B. A. Crouch, and J. G. Williams, *Polym. Eng. Sci.,* **30,** 241–248 (1990).
5. *Design Handbook for DuPont Engineering Plastics, Module II,* DuPont (1993).
6. P. E. Bretz, R. W. Hertzberg, and J. A. Manson, *J. Mater. Sci.,* **16,** 2061 (1981).
7. J. Karger-Kocsis and K. Friedrich, *Plast. Rubber Process. Appl.,* **12,** 63 (1989).
8. S. Michielsen, *J. Mater. Sci. Lett.,* **11,** 982–984 (1992).
9. J. G. Williams, *Fracture Mechanics of Polymers,* Wiley, New York, 1984.
10. D. P. Rooke and D. J. Cartwright, *Compendium of Stress Intensity Factors,* Her Majesty's Stationery Office, London, 1976.

Received July 7, 1993
Accepted November 20, 1993